Light-induced diffusion and desorption of alkali metals in a siloxane film: Theory and experiment

S. N. Atutov,* V. Biancalana, P. Bicchi, C. Marinelli, E. Mariotti, M. Meucci, A. Nagel,† K. A. Nasyrov,* S. Rachini, and L. Moi

INFM and Dipartimento di Fisica dell'Università degli Studi di Siena, Banchi di Sotto 55, I-53100 Siena, Italy

(Received 29 October 1998; revised manuscript received 30 June 1999)

The light-induced desorption and diffusion of alkali-metal atoms in organic films are interesting fields of investigation. An impressive demonstration is given by the recently observed light-induced atomic desorption (LIAD) effect, where a huge alkali-metal atom desorption from siloxane films, previously exposed to atomic vapors, is induced by weak and nonresonant light. In this paper, experimental data and a one-dimensional theoretical model of the effect are presented. The model gives a good description of the vapor density dynamics by taking into account both the atomic diffusion inside the coating and the surface desorption. General equations are reported and discussed within the limits of experimental interest. The potential barrier at the vapor-surface interface and the activation energy for Rb in (poly)dimethylsiloxane have been determined. [S1050-2947(99)01512-7]

PACS number(s): 34.50.Dy, 79.20.La

I. INTRODUCTION

The atomic diffusion inside dielectrics and the atomic adsorption-desorption processes are interesting fields of investigation as they give useful insights into both the knowledge of atom-dielectric interactions and to important practical applications. They have been recently enriched by the observation of new phenomena connected to the presence of light. We have studied both experimentally and theoretically the influence of light on the diffusion and on the adsorption-desorption rates of alkali-metal atoms in siloxane films deposited on a Pyrex substrate. We show that nonresonant light increases both the mobility of the atoms inside the coating and the desorption rate. The dependence of the adsorbed atom diffusion on the light frequency and on the light intensity is demonstrated. Its dependence on the cell temperature has been studied as well. These experiments follow the recent and unexpected observation of a new effect consisting of a huge atomic desorption from transparent silane films when weak and incoherent visible light shines the surface. The effect, named LIAD (i.e., light-induced atomic desorption) [1], has been observed and experimentally investigated by Gozzini *et al.* [2] with Na atoms, by Meucci *et al.* with Rb atoms [1], and by Mariotti *et al.* with Cs atoms [3]. In all these experiments the film, which coats the inner surface of the resonance cells, was made from an ether solution either of a polymer, namely the (poly)-dimethylsiloxane (PDMS) [1,2], or of a crown molecule, namely the octamethylcyclotetrasiloxane (OCT) [3]. Photodesorption of Na_2 molecules has also been observed [4]. The analysis of the desorption dynamics gives important information on LIAD and it has been studied with Rb adsorbed on PDMS [5]. An efficient atomic source of rubidium controlled by light has been realized [6]. By using a resonant laser beam as a probe, LIAD is made visible to the naked eye as the vapor density, and hence the fluorescence intensity, may change by many orders of magnitude with respect to the thermal equilibrium value.

LIAD is a nonthermal effect and has no relation with those desorption phenomena driven by powerful laser pulses, which produce a brute local heating of the substrate and surface ablation. LIAD of Rb and Cs is even produced by the light emitted by a pocket lamp and also at very low cell temperatures [1]. It shows a frequency threshold analogous to the work function of the photoelectric effect in metals [2] and, similarly, an increasing efficiency with increasing light frequency [1,2,4]. All these interesting features have to be completed by recalling that the siloxane films have been used and studied in the past in optical pumping [7] and light-induced drift [8] experiments because of their very weak adsorption energy E_{ads} and negligible atom-surface interaction. As a consequence, atomic surface density assumes very low values making unlikely the formation of a metallic monolayer or of clusters on the surface itself.

A tentative interpretation of LIAD at the microscopic scale has been proposed for sodium adsorbed on PDMS [2,4]. According to that approach, sodium atoms are solvated in the siloxane compound and the Na^+PDMS^- and $Na_2{}^+PDMS^-$ complexes are formed. The light induces a reverse mechanism which brings back atoms and molecules in the vapor phase. This approach explains the observed threshold in the excitation light spectrum but it leaves unsolved a number of important questions such as, for example, the influence of the coating molecular structure [3], and the dependence on the temperature and on the buffer gas pressure. In disagreement with our experimental evidence, LIAD is strictly correlated to the specific chemical properties of siloxanes. Moreover, LIAD is confined to the surface effect category while we show that diffusion inside the coating plays a major role.

We report experimental data and we show that a self-

*Permanent address: Institute of Automation and Electrometry, Novosibirsk 90, Russia.

†Permanent address: Institut für Angewandte Physik, Wegelerstrasse 8, Bonn, Germany.

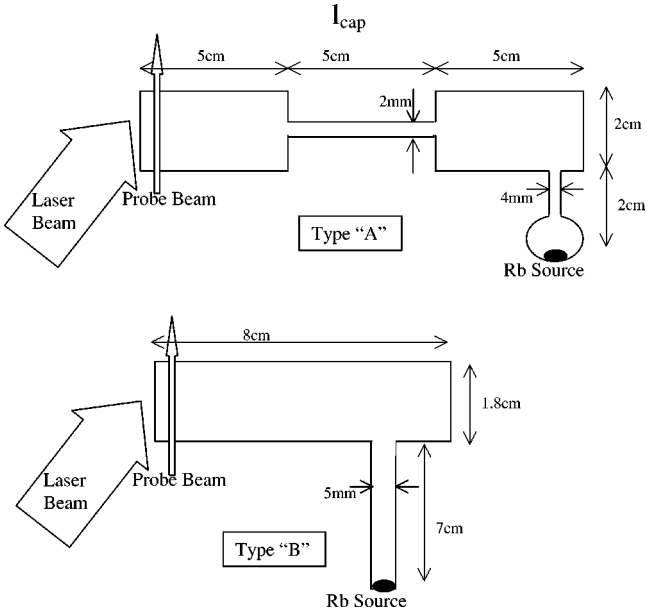

FIG. 1. Sketch of two resonance cells used in the experiments. Numbers express their actual size. All cells were coated with PDMS.

consistent picture of the LIAD phenomenon needs not only the increase in the desorption rate at the surface, but also diffusion in the coating bulk. In fact, light increases the diffusion in the coating bulk so that LIAD can be interpreted as a light-induced enhancement of atom mobility. These assumptions are also supported by the 1D model we developed. We find that the diffusion dynamics inside the coating drives the time evolution of the rubidium density in the gas phase. Therefore, we get the important result that LIAD is mostly a bulk effect and not only a surface effect. Moreover, we have evidence, after some preliminary measurements, that LIAD is not confined to the specific chemical properties of the siloxanes but it is a more general effect.

II. EXPERIMENTAL SETUP AND SILOXANE FILM PREPARATION

The light-induced diffusion and desorption of Rb atoms adsorbed in PDMS is studied using, as desorbing light, the radiation from an Ar^+ laser tuned to $\lambda_1 = 458$ nm or $\lambda_2 = 514$ nm, and from a Ti-sapphire laser tuned to $\lambda_3 = 800$ nm. The diameter of the laser beams is enlarged by a telescope in order to achieve a complete illumination of the end window of the cells or of the whole cells (see Fig. 1). The light power density I_L in the experiment ranges from 1×10^{-3} W/cm^2 to 30×10^{-3} W/cm^2. A diode laser, tuned to the Rb D_2 absorption line ($\lambda_{probe} = 780$ nm), is used to probe the vapor density. It crosses the cell in a direction parallel to the cell entrance window and it is strongly attenuated down to a few microwatts in order to avoid both perturbation of the cell surface and optical pumping of atoms. The laser frequency is scanned through the absorption line at about 100 Hz rate. The evolution of the vapor density is obtained by measuring the fraction of the probe diode laser light transmitted through the cell. The light absorption is measured by the box-car technique with the gate exactly located on the maximum of the strongest Rb hyperfine line component ($F=3$ ground level of ^{85}Rb isotope). When higher atomic densities are achieved causing the probe beam to be completely absorbed in that component, the weakest hyperfine transition from the $F=1$ ground level of ^{87}Rb isotope is used. Experimental studies showed that no isotopic effects are visible, allowing a free choice of the line. The absorption signals are stored and processed by a digital oscilloscope and by a personal computer. The Rb density variation is calculated taking into account Beer's exponential absorption law. This acquisition system allows us to collect data with 10 ms resolution limit over several hours and to measure density variation of Rb vapor in a wide range. The absolute Rb vapor density in equilibrium with a metal reservoir is estimated from the temperature of the source metal drop, once provided a steady-state vapor concentration [9].

In order to analyze the LIAD dynamics and to make a comparison with the proposed diffusion model, several coated Pyrex glass cells with different shapes, sizes, and buffer gas pressures have been used. In Fig. 1, two of these cells are sketched and the relevant dimensions reported. The ''*A*''-type cell consists of two cylinders connected by a capillary. One of them is linked to the Rb reservoir, thus metal vapor can reach the other cylinder only through the capillary. The ''*B*''-type cell consists of one cylinder directly connected to the Rb source through a capillary. These two different cell shapes realize very different path lengths of the photodesorbed atoms to the alkali-metal reservoir giving useful insights into the diffusion and adsorption-desorption processes.

Even if the coating preparation has been described in detail in previous papers (see for example, Ref. [1]), it might be helpful to recall here the standard procedure. The organic film is made by rinsing the cell with an ether solution of a few percent of PDMS compound. When the ether is evaporated, the cell is placed in an oven at 200 °C for several hours and then connected to a turbo pump for several days to eliminate traces of chemical active impurities that might be present inside of coating. It is better to warm up the cell in order to improve and speed up this cleaning process. The cell is then filled by a buffer gas at a chosen pressure and, by gently warming up the cell, a melted Rb metal drop is distilled in the cell reservoir. It is important to note that, in order to avoid contamination of the cell and poisoning of the effect due to unwanted chemical reactions between hot metal drops and the organic compound, the reservoir bulb is not coated.

III. THEORY: THE 1D DIFFUSION MODEL

We assume that Rb atoms are spreaded in the coating where they occupy interstitial positions. In the absence of light, Rb atom diffusion can be described by the Arrhenius relation

$$D_0 \propto e^{-E_{act}/k_B T}. \tag{1}$$

E_{act} is the activation energy characterizing the depth of the potential wells where atoms are located, k_B is the Boltzmann constant, and T is the temperature. When the desorbing light is on, diffusion changes and, assuming a linear dependence on the light intensity I_L, the diffusion coefficient becomes

$$D_c = D_0 + D_1(\lambda, I_L) = D_0 + d(\lambda) I_L , \tag{2}$$

where D_c is the diffusion coefficient in the presence of light, D_1 is the contribution from excited atoms only, and $d(\lambda)$ is a coefficient which depends on the wavelength of desorbing light.

Atoms close to the coating surface can leave it and get into the cell bulk where their diffusion coefficient D_{gas} is inversely proportional to the buffer gas pressure p. At the same time, atoms from the gas phase can get adsorbed again. This dynamical situation can be described by considering the atom fluxes in the two directions. The flux of atoms leaving the surface can be written in the form

$$J^+ = \alpha N, \tag{3}$$

where N is the atomic density in the coating; α has the dimensions of a velocity and characterizes the atomic desorption rate. Similarly to Eq. (2), the atom desorbing rate α can be written, at a fixed temperature, as

$$\alpha = \alpha_0 + \alpha_1(\lambda, I_L) = \alpha_0 + k(\lambda) I_L , \tag{4}$$

where α_0 is the desorption rate in the dark (thermal desorption rate) and $k(\lambda)$ is a function of the light wavelength only.

In order to complete this physical picture, the flux of thermal atoms in the opposite direction, i.e., from the vapor to the coating, has to be taken into account. The flux of adsorbed atoms can then be expressed as follows:

$$J^- = -\beta n, \tag{5}$$

where n is the atomic density in the vapor phase; β has the dimensions of a velocity and it characterizes the adsorbing rate. The ratio β / v_T, where v_T is the mean thermal velocity, gives the probability the atoms have to be adsorbed when they collide on the coated wall. It is important to remark that in our experiment the frequency of the desorbing light is always far away from the Rb resonance absorption lines in the vapor phase. Therefore, we can assume that β does not depend on light intensity and frequency. The total flux of atoms through the surface is then given by

$$J = J^+ + J^- = \alpha N - \beta n. \tag{6}$$

In the absence of the desorbing light, the sum of these two fluxes must be equal to zero, i.e., $J = 0$. Hence, when the equilibrium in the dark is considered, the atomic concentrations N_0, in the coating, and n_0, in the gas phase, have to satisfy the following condition:

$$N_0 = \frac{\beta}{\alpha_0} n_0 . \tag{7}$$

Experimental evidence shows that $N_0 \gg n_0$ [1,2], as qualitatively sketched in Fig. 2, and hence $\beta \gg \alpha_0$.

When the desorbing light is switched on, the vapor density dynamics can be described by the following equation:

$$\frac{dn}{dt} = \frac{J}{L} - \gamma (n - n_0), \tag{8}$$

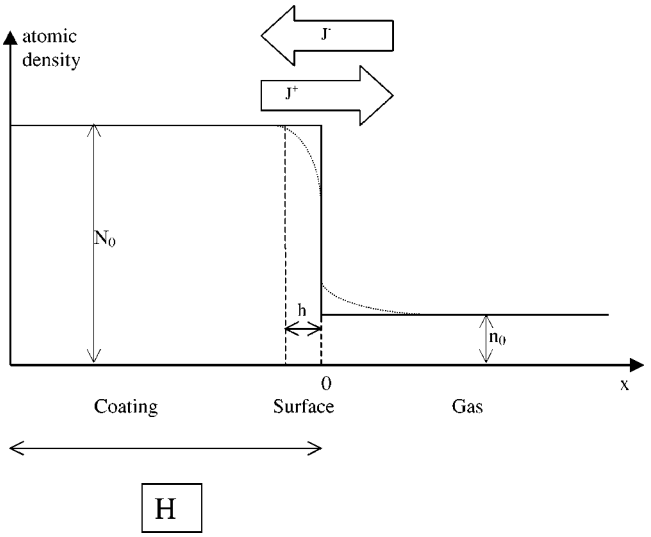

FIG. 2. Sketch of the diffusion processes at the vapor-surface interface. J^+ represents the atomic flux from the coating to the gas phase; J^- is the flux of atoms from the gas into the coating; H is the coating thickness; h is defined in the text.

where $L = V/S$ is the characteristic cell length, V is the volume of the cell, and S is its surface. The last term of Eq. (8) describes the vapor density relaxation back to the thermal equilibrium density in the dark controlled by Rb source; γ^{-1} is the relaxation characteristic time. For the sake of simplicity, no diffusion process in the gas phase has been taken into account while deriving Eq. (8). Therefore, this equation is valid as long as the vapor density can be considered independent of the spatial coordinates, i.e., $n(x,t) = n(t)$. This means that Eq. (8) properly describes only processes evolving with a characteristic time longer than $\tau_{\text{gas}} = L^2 / D_{\text{gas}}$. In our experimental condition, τ_{gas} is in the order of a fraction of a second. For $t < \tau_{\text{gas}}$, Eq. (8) should be replaced by a diffusion equation.

On the other hand, the spatial concentration gradient inside the coating cannot be neglected because the diffusion coefficient is much smaller than in the gas phase [10]. As the illuminated surface is much larger than the coating thickness H, the atomic density evolution inside the coating can be described by the one-dimensional diffusion equation

$$\frac{\partial N}{\partial t} = D_c \frac{\partial^2 N}{\partial x^2} . \tag{9}$$

The boundary conditions

$$-D_c \frac{\partial N}{\partial x}(0) = J \tag{10}$$

at the vapor-surface interface $(x = 0)$

$$D_c \frac{\partial N}{\partial x}(-H) = 0 \tag{11}$$

at the coating-substrate interface $(x = -H)$ hold. This last assumption is valid, at a given temperature, if we assume that the cell is old enough that the pyrex substrate is saturated by Rb atoms. The opposite situation would be that

atoms are continuously lost in the glass where they are irreversibly adsorbed. Even if any intermediate situation is plausible, as this boundary condition has a small effect on our description and only when very long time scale dynamics is considered, we do not stress this point here any further.

We show that this model is correct and it is able to reproduce the main features of the LIAD effect. Let us therefore consider two opposite cases which allow us to obtain an analytical solution of the equations. They correspond to the low and the high desorbing light intensity limits, respectively.

A. Weak desorbing light intensity

The light intensity I_L is assumed weak enough to induce a negligible change of the atomic density N near the coating surface. This condition allows us to impose that $N(x=0) \cong N_0$, where N_0 is the atomic density inside the coating in the absence of light and at the thermal equilibrium. Equation (8) then becomes

$$\frac{dn}{dt} = \frac{\alpha N_0}{L} + \gamma n_0 - \left(\gamma + \frac{\beta}{L}\right) n \tag{12}$$

and its solution is

$$n(t) = n_0 + \frac{\alpha_1 N_0}{\beta + \gamma L}[1 - e^{-[\gamma + (\beta/L)]t}]. \tag{13}$$

It is clear from this solution that, by switching on the desorbing light, the atomic density n increases linearly with time and attains its maximum $n_{\max}^{\text{weak}}$ value, which corresponds to a new steady-state regime, roughly after the characteristic time τ_1 given by

$$\tau_1^{-1} = \gamma + \frac{\beta}{L}.$$

The maximum density deviation $\Delta n_{\max}^{\text{weak}}$ is

$$\Delta n_{\max}^{\text{weak}} = n_{\max}^{\text{weak}} - n_0 = \frac{\alpha_1}{\beta + \gamma L} N_0 = \frac{n_0}{\alpha_0} \frac{\beta}{L} \tau_1 k(\lambda) I_L . \tag{14}$$

Equation (13) is valid only for a short time interval Δt after the desorbing light has been switched on. Upon these assumptions LIAD is driven only by the gas dynamics as the coating is negligibly affected by light. In fact, only a small fraction of the atoms confined within a thickness $h = \sqrt{D_c \tau_1}$ is expected to be desorbed. The vapor density increase then depends on the relaxation time of the vapor density back to the thermal equilibrium: it is longer this time the larger the number of atoms accumulated in the gas phase.

When $t \gg \tau_1$, the slow decreasing of the atomic density close to the inner coating surface ($h \leqslant x \leqslant 0$) has to be taken into account. By considering that the desorption process, for $t \gg \tau_1$, is very small and almost stationary, it is allowed to impose in Eq. (8) the condition $dn/dt = 0$. With the help of Eq. (6), n as a function of $N(0,t)$ can be found,

$$n(t) = \frac{\alpha N(0,t) + \gamma L n_0}{\beta + \gamma L}. \tag{15}$$

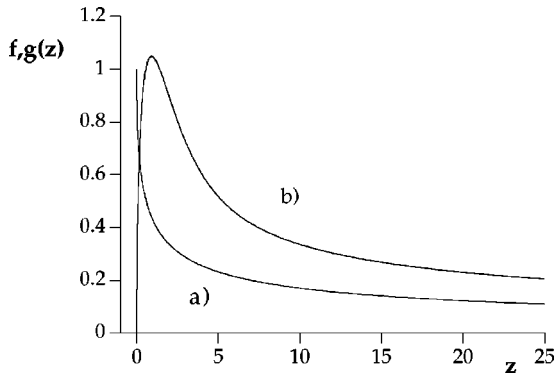

FIG. 3. Plots of (a) $f(z)$ and (b) $g(z)$ functions.

Using this equation, the boundary condition (10) may be written in the form

$$-D_c \frac{\partial N}{\partial x}(0) = \gamma \tau_1 [\alpha N(0,t) - \beta n_0]. \tag{16}$$

The solution of Eq. (9) for $n(t)$ with the boundary condition (16) and for $\tau_1 \ll t < \tau_d = H^2/D_c$, where τ_d is the characteristic diffusion time inside the coating, can be obtained after applying the Laplace transformation,

$$n(t) - n_0 = \Delta n_{\max}^{\text{weak}} f\left(\frac{t}{\tau_2}\right), \quad \tau_2 = \frac{D_c}{(\gamma \tau_1)^2 \alpha^2}, \tag{17}$$

where

$$f(z) = e^z \operatorname{erfc}(\sqrt{z}). \tag{18}$$

The function $f(z)$ is shown in Fig. 3(a). $f(z)$ decreases with z and, when $z \gg 1$, goes as $f(z) \sim 1/\sqrt{z}$.

When $t \gg \tau_d$, not only the coating surface but the whole coating gives its contribution as a sole atomic source, and instead of Eq. (9), the following balance equation can be used:

$$H \frac{dN}{dt} = J = \gamma \tau_1 (\alpha N - \beta n_0). \tag{19}$$

This equation gives the asymptotic behavior of $n(t)$,

$$n(t) - n_0 \propto e^{-t/\tau_3}, \quad \tau_3 = \frac{H}{\alpha} \frac{1}{\gamma \tau_1}. \tag{20}$$

To summarize, we have shown that upon weak light illumination, LIAD presents three different regimes: (i) immediately after the light has been switched on, Δn increases linearly; (ii) then Δn reaches a maximum and starts slowly decreasing. The density decay is governed by the $f(z)$ function until $t \cong \tau_d$; (iii) for longer time, $n(t)$ decreases exponentially back to the equilibrium value n_0.

An important issue is to determine when the limit of weak light intensity becomes not valid. This approximation is not correct when, for $t \leqslant \tau_1$, the atomic density variation ΔN in the coating layer close to the surface and of thickness $h = \sqrt{D_c \tau_1}$ becomes comparable to N_0. This density variation ΔN gives rise to the atomic density change $\Delta n_{\max}$ in the gas phase equal to

$$h\Delta N = L\Delta n_{\max} = \alpha_1 \tau_1 N_0 . \tag{21}$$

From this condition it can be derived that the weak intensity approximation (i.e., $\Delta N \ll N_0$) is correct if

$$\alpha_1 < \alpha_S = \sqrt{\frac{D_c}{\tau_1}}, \tag{22}$$

where α_S can be considered as the saturation parameter of α_1. It is important to remark that in this case α_S depends on the diffusion coefficient of the atoms inside the coating.

B. High desorbing light intensity

When the desorbing light intensity I_L is so high that all atoms in the region close to the surface are instantaneously desorbed into the cell volume, it holds that

$$N(0,t) \cong 0, \quad t > 0. \tag{23}$$

Equation (9) with the new boundary condition (23) gives the flux of atoms from the coating

$$J = N_0 \sqrt{\frac{D_c}{\pi t}} \tag{24}$$

and, by using Eqs. (8) and (24), $n(t)$ as a function of time becomes

$$n(t) - n_0 = \frac{N_0}{L} \sqrt{\frac{D_c}{\pi \gamma}} g(\gamma t), \tag{25}$$

where the function $g(z)$ is

$$g(z) = e^{-z} \int_0^z \frac{e^{\zeta}}{\sqrt{\zeta}} d\zeta. \tag{26}$$

A plot of $g(z)$ is shown in Fig. 3(b). From Eqs. (25) and (26) it results that $\Delta n(t)$ increases, for $0 < t < \gamma^{-1}$, as

$$\Delta n(t) \approx \frac{2N_0}{L} \sqrt{\frac{D_c t}{\pi}}. \tag{27}$$

It gets its maximum

$$\Delta n_{\max}^{\text{high}} = \frac{N_0}{L} \sqrt{\frac{D_c}{\pi \gamma}} \tag{28}$$

at $t = \gamma^{-1}$ and then it starts slowly decreasing for $t > \gamma^{-1}$ according to

$$\Delta n(t) \cong \frac{N_0}{L} \sqrt{\frac{D}{\pi \gamma}} \frac{1}{\sqrt{\gamma t}} = \frac{1}{\sqrt{\gamma t}} \Delta n_{\max}^{\text{high}}. \tag{29}$$

Therefore the main features upon very strong light intensity illumination can be summarized as follows: (i) at the beginning $\Delta n(t)$ increases as $\sqrt{t}$; (ii) $\Delta n(t)$ reaches the maximum density deviation $\Delta n_{\max}^{\text{high}}$; (iii) then the vapor density at long delay times decreases as $1/\sqrt{t}$. $\Delta n_{\max}^{\text{high}}$ is limited by the diffusion coefficient of the atoms inside the coating. This means that, at extremely high light intensity, the total number of atoms that can be desorbed from the coating is limited by the diffusion of fresh atoms from the bulk to the surface of the coating. This model has been developed by assuming that the whole cell surface is illuminated by the desorbing light. When, however, in the experiment only a part of the cell is illuminated and a large fraction remains in the dark, we assume that this last can adsorb the excess of atoms desorbed by the illuminated one. In this case, Eq. (8) has to be modified as

$$\frac{dn}{dt} = \frac{S^{(\text{ill})}}{V} J^{(\text{ill})} + \frac{S^{(\text{dark})}}{V} J^{(\text{dark})} - \gamma (n - n_0), \tag{30}$$

where $S^{(\text{ill})}$ and $S^{(\text{dark})}$ are the illuminated and not illuminated surfaces, respectively, and

$$J^{(\text{ill})} = \alpha N^{(\text{ill})}(0) - \beta n, \quad J^{(\text{dark})} = \alpha_0 N^{(\text{dark})}(0) - \beta n$$

are the fluxes from the illuminated and not illuminated parts, respectively.

The solution of Eq. (9) for both illuminated and not illuminated parts has to be found and this can be done with numerical simulation. The results show no substantial changes with respect to the simpler case previously discussed.

IV. EXPERIMENTAL RESULTS AND DISCUSSION

In order to verify the theoretical model and the role of the atomic diffusion inside the siloxane film, a series of experiments has been performed.

A. LIAD as a function of time

The cylinder of the *A*-type cell not connected with the metal reservoir has been illuminated and the absorption signal has been detected. The vapor density has been evaluated by applying Beer's law. In order to make a comparison with the model, the ratio between the vapor density variation and the vapor density at the thermal equilibrium n_0, i.e., $\Delta n(t)/n_0$, has been plotted.

Figure 4(a) shows several plots of $\Delta n(t)/n_0$ as a function of time for different desorbing laser power. The desorbing laser wavelength is $\lambda_3 = 800$ nm. $\Delta n(t)/n_0$ increases with the laser intensity and shows, as predicted by the theoretical model, a different time dependence. At relatively weak intensities and immediately after the light has been switched on, $\Delta n(t)/n_0$ is linearly increasing with time *t*. By further increasing the light intensity, the linear dependence on *t*, according to the model, shifts to a $\sqrt{t}$ dependence. The passage from low to high light intensity is observable in the experiment.

In Fig. 4(b), the (a) and (e) signals of Fig. 4(a) are shown after their renormalization. The two dashed curves give the best fit. The signal (e) is fitted by a linear function on *t*, while signal (a) by a square root function of *t*.

From Fig. 4, the characteristic time $\tau_1 = (\gamma + \beta/L)^{-1}$ can be evaluated and its value is $\tau_1 = 30$ s. The relaxation time of Rb density in the illuminated cylinder of the *A* cell is controlled by the diffusion of the atom through the capillary towards the second cylinder connected to the metallic source. This time is

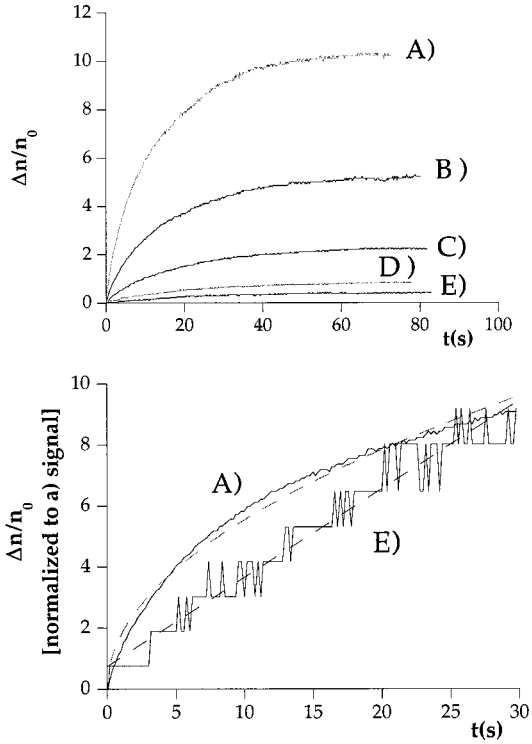

FIG. 4. (a) $\Delta n/n_0$ as a function of time. The curves correspond to different laser power. $I_L=$ (A) 181 mW; (B) 51.7 mW; (C) 12.4 mW; (D) 2.0 mW; (E) 0.78 mW (see text). (B), (A), and (E) curves renormalized. The broken lines give the best fit of the two curves. (Desorbing light wavelength $\lambda=800$ nm.)

$$\gamma^{-1}=Vl_{\mathrm{cap}}/(S_{\mathrm{cap}}D_{\mathrm{gas}}),$$

where l_{cap} and S_{cap} are the length and the cross section of the capillary, and D_{gas} is the diffusion coefficient of Rb atoms in the Ar buffer gas filling the cell. For 10 torr of argon pressure, $D_{\mathrm{gas}}\cong 10$ cm^2/s and γ^{-1} is about 250 s. As $\gamma^{-1}\gg\tau_1$ and $\tau_1^{-1}\cong\beta/L$ it follows that $\beta=3\times10^{-2}$ cm/s for $L=1$ cm.

It is now possible to evaluate the probability $\kappa=\beta/v_T$ of Rb atoms to be adsorbed by PDMS coating in the collision with the surface, $\kappa\cong10^{-6}$. This very small value confirms the results obtained in optical pumping and light-induced drift experiments and makes very unlikely the hypothesis that LIAD can only be a surface effect.

B. LIAD as a function of the laser intensity

$\Delta n_{\max}/n_0$ as a function of the desorbing light intensity is shown in Fig. 5(a). At low intensity, according to Eq. (14), $\Delta n_{\max}/n_0$ is proportional to the light power P_L. By increasing P_L, a deviation from linearity is observed and $\Delta n_{\max}/n_0$ shows a dependence on $\sqrt{P_L}$. This is better seen in Fig. 5(b), where the $(\Delta n_{\max}/n_0)^2$ data for the different wavelengths are renormalized and plotted versus P_L. The solid line curve gives the linear fit.

According to Eq. (28), in the high-intensity limit, $\Delta n_{\max}/n_0$ is proportional to $\sqrt{D_c}$. Therefore, if the diffusion coefficient would not depend on the desorbing light intensity, $\Delta n_{\max}/n_0$ should saturate and remain constant. It means that at extremely high light intensity, the total number of atoms

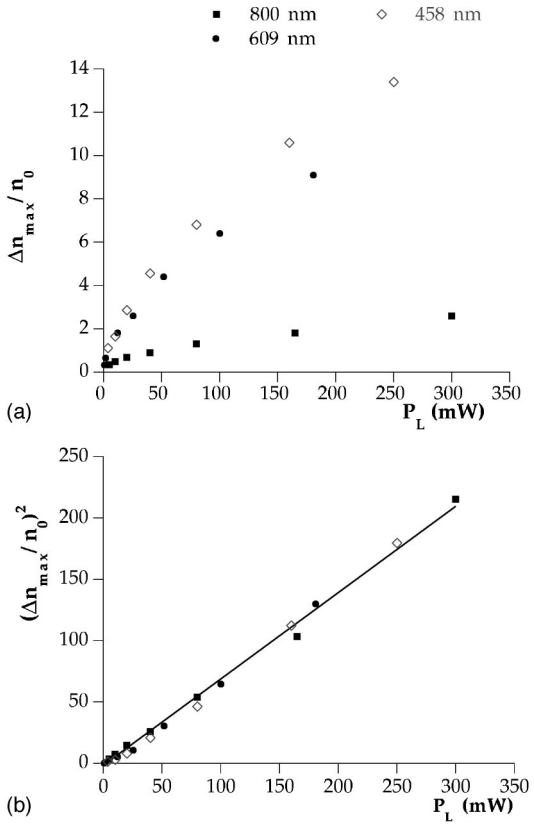

FIG. 5. (a) $\Delta n_{\max}/n_0$ as a function of the laser power for different desorbing light wavelengths. (b) $(\Delta n_{\max}/n_0)^2$ as a function of the laser power. The signals have been renormalized to show their similar dependence on P_L. The solid line shows the best fit. A linear dependence on P_L is evident.

that could be desorbed from the surface should be limited by the diffusion of fresh atoms from the bulk to the surface in such a way as to replace the desorbed ones. The fact that the experimental results show at high light intensity a square root dependence on P_L of $\Delta n_{\max}/n_0$ demonstrates that the diffusion coefficient D_c is proportional to the light intensity I_L. This result supports once more our model based on the light-induced diffusion of Rb atoms inside the coating.

C. LIAD as a function of buffer gas pressure

Two *B*-type cells, of the same size but filled with two different buffer gas pressures, namely 3.5 torr (cell I) and 35 torr (cell II), have been illuminated by the same high-intensity light. The $\Delta n(t)/n_0$ as a function of time is reported in Fig. 6 for the two cells. Both signals increase at the beginning with the square root of time, but they reach the maximum at different times.

In the low pressure cell, $\Delta n(t)^{(\mathrm{I})}/n_0$ gets its maximum value at $\tau^{(\mathrm{I})}\cong4$ s. The $\Delta n(t)^{(\mathrm{II})}/n_0$ instead continues to increase and gets its maximum at $\tau^{(\mathrm{I})}\cong50$ s. This result is qualitatively in agreement with the model. In fact, the time γ^{-1} needed to reach the maximum density is proportional to the buffer gas pressure p and, as measured, $\tau^{(\mathrm{II})}/\tau^{(\mathrm{I})}\cong10$. Moreover, according to Eq. (28), $\Delta n_{\max}/n_0$ is proportional to $1/\sqrt{\gamma}\propto\sqrt{p}$ and it should be

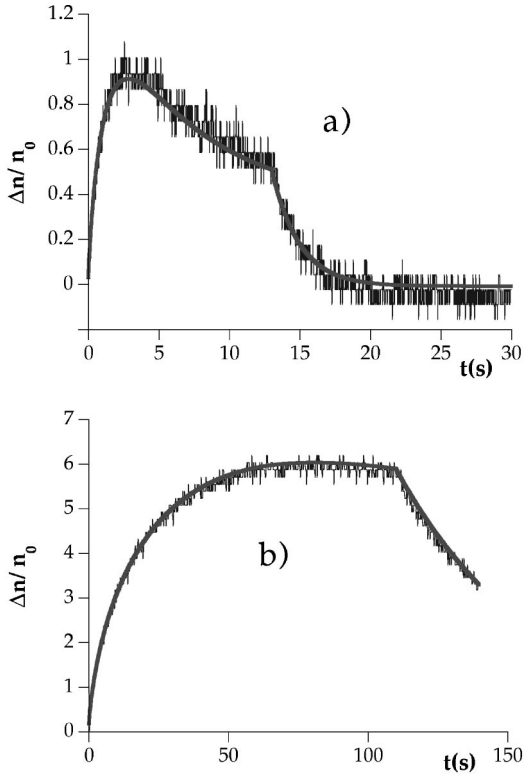

FIG. 6. $\Delta n/n_0$ as a function of time in the presence of two different buffer gas pressures: (a) $p=3.5$ torr; (b) $p=35$ torr. Solid curves represent the best fit according to the model.

$$\frac{\Delta n_{\max}^{(\mathrm{II})}/n_0}{\Delta n_{\max}^{(\mathrm{I})}/n_0}=\sqrt{\frac{p^{(\mathrm{II})}}{p^{(\mathrm{I})}}},$$

which is in qualitative agreement with the experiment. We remind the reader that as the experiments have been made in two distinct cells, the behavior cannot be exactly the same as the coating thickness cannot be well controlled.

The $\Delta n(t)^{(\mathrm{I,II})}/n_0$ signals presents precisely the same features as the theoretical curve $g(\gamma t)$ plotted in Fig. 3(b). From this it is found $\gamma p=1.7\ \mathrm{s}^{-1}$ torr for the *B*-type cells.

D. LIAD as a function of temperature

The same two *B*-type cells have been arranged inside a cryostat transparent to both the desorbing and the probe laser light. In Fig. 7, $\Delta n_{\max}^{(\mathrm{I,II})}/n_0$ values as a function of T are reported.

For weak desorbing light intensity, when $D_0 > D_1(\lambda, I_L)$, the diffusion of the atoms inside the coating can be described by the Arrhenius relationship $D_0 \propto e^{-E_{\mathrm{act}}/(k_B T)}$ that corresponds to the atom diffusion in the dark. This means that the saturation parameter $\alpha_S=\sqrt{D_c/\tau_1} \sim e^{-E_{\mathrm{act}}/(2k_B T)}$ [see Eq. (22)] also depends on the temperature. Thus, at fixed light intensity and consequently at fixed α_1, by changing the temperature of the cell it is possible to shift the experiment from the high-intensity limit ($\alpha_1 > \alpha_S$) at low temperatures to the low-intensity limit ($\alpha_1 < \alpha_S$) at relatively high temperatures.

In Fig. 7(a), $\Delta n_{\max}^{(\mathrm{I,II})}/n_0$ curves are normalized in such a way that the presence of a shift of the transition temperature towards higher values of T becomes evident for lower pressures as predicted by the model. The shift value is in quantitative agreement with the prediction.

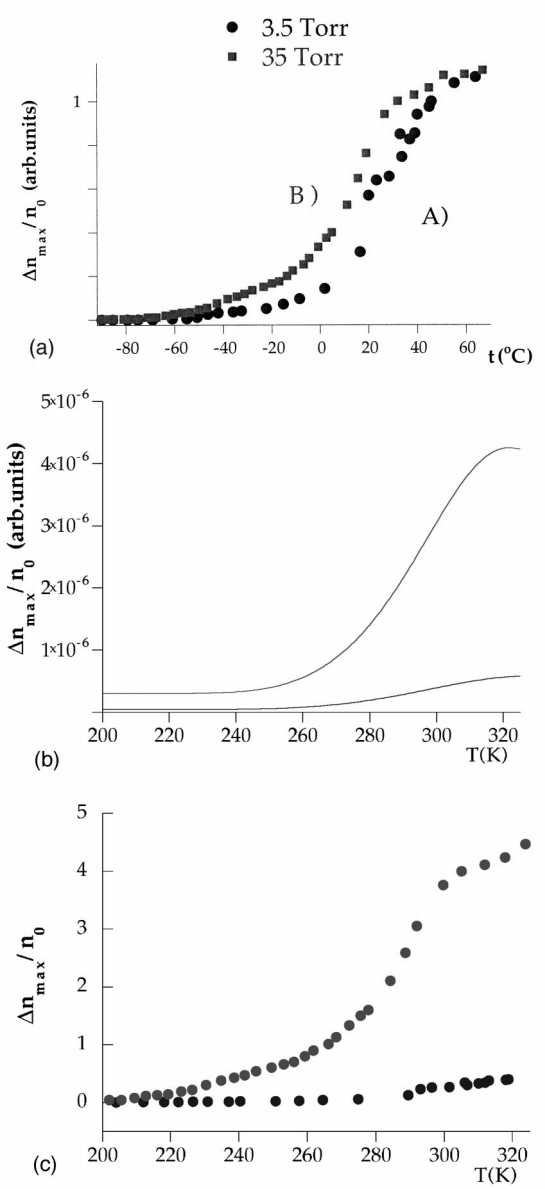

FIG. 7. (a) $\Delta n_{\max}/n_0$ as a function of the cell temperature. Curve (A) corresponds to the cell filled with 3.5 torr of argon and curve (B) to that filled with 35 torr of argon, normalized to each other. (b) is a simulation on the base of the model; (c) is the experimental behavior in the correct ratio.

According to Eq. (28), at low temperatures when the high-intensity limit is valid, $\Delta n_{\max}/n_0$ is proportional to $\sqrt{D_c/\gamma}$. From this fact, two consequences follow. The first one is that $\Delta n_{\max}/n_0$ has to increase with the temperature as $e^{-E_{\mathrm{act}}/(2k_B T)}$ until the high-intensity limit is replaced by the low-intensity limit. The second one is that, as $\Delta n_{\max}$ is proportional to $\sqrt{p}$, it has to be true for the two cells that $\Delta n_{\max}^{(\mathrm{II})}=(p_2/p_1)^{1/2}\Delta n_{\max}^{(\mathrm{I})}=\sqrt{10}\Delta n_{\max}^{(\mathrm{I})}$ at the high-intensity limit. Both these facts are verified in Figs. 7(b) and 7(c), where a comparison between the model based evaluation and the experimental results without normalization is given. The curves reproduce very well the behavior and give the correct ratios for the density variations at a fixed temperature.

At relatively high temperatures, when the low-intensity limit is valid, $\Delta n_{\max}/n_0$ depends on α_1 only [see Eq. (14)] and does not depend on the temperature. Therefore, as it can be seen from Fig. 7, at high temperatures $\Delta n_{\max}/n_0$ reaches a saturation value.

From these measurements, the activation energy E_{act} can be derived and it results $E_{\text{act}}=(0.7\pm0.1)$ eV. We have evaluated both the activation energy E_{act} and the adsorption probability κ of Rb atoms in PDMS. From κ it is possible to evaluate E_{chem}, i.e., the potential barrier the Rb atoms have to overcome to get inside the coating,

$$E_{\text{chem}}=-k_B T\ln(\kappa)=0.37\ \text{eV}.$$

Due to the incertitude of the atomic density value inside the coating, it is not possible to derive from the experiment the desorption energy E_{des} and the atomic diffusion coefficient. The characteristic diffusion time τ_d of the atoms inside the coating also remains undetermined. Rough estimates of τ_d give values ranging within several decades around 10^5 s. Because of these problems, we restrict ourselves in this work to the investigation of LIAD in the limit of short illumination time.

V. CONCLUSION

In conclusion, we have developed a simple model of the light-induced atomic desorption effect based on the diffusion processes of atoms in both coating and cell volume and we have made experimental tests of the model predictions. We have shown that the model not only describes the main features of the effect showing good agreement with the experimental data, but it also gives some more general insights. In fact, we infer from our data that neutral atoms and not ions are diffusing inside the coating and that LIAD should be observable also with other completely different coatings. We have, for example, evidence of Rb atom desorption from surfaces prepared with a liquid film of common mineral oils. Moreover, by using buffer gas pressures higher than the atmospheric one, it should be possible to detect the LIAD effect in solid bulks or detect a very weak effect at temperatures close to the absolute zero. It can be very interesting, for example, to analyze systems characterized by relatively weak surface bonding energy and large diffusion, as it is for Li atoms solved in germanium [10].

ACKNOWLEDGMENTS

We would like to acknowledge the technical help of M. Badalassi, E. Corsi, V. Gabbani, A. Marchini, A. Pifferi, and C. Stanghini. We are grateful to A. Kopystynska, A. M. Shalagin, and G. Nienhuis for their contribution and discussion. This work has been partially supported by the INFN and EC [Contract No. CHRX CT93 0366(rep792)].

[1] M. Meucci, E. Mariotti, P. Bicchi, C. Marinelli, and L. Moi, Europhys. Lett. **25**, 639 (1994).
[2] A. Gozzini, F. Mango, J. H. Xu, G. Alzetta, F. Maccarrone, and R. A. Bernheim, Nuovo Cimento D **15**, 709 (1993).
[3] E. Mariotti, M. Meucci, C. Marinelli, P. Bicchi, and L. Moi, in *Proceedings of the XII International Conference on Laser Spectroscopy*, edited by M. Inguscio, M. Allegrini, and A. Sasso (World Scientific, New York, 1996), p. 390.
[4] J. H. Xu, A. Gozzini, F. Mango, G. Alzetta, and R. A. Bernheim, Phys. Rev. A **54**, 3146 (1996).
[5] E. Mariotti, S. Atutov, M. Meucci, P. Bicchi, C. Marinelli, and L. Moi, Chem. Phys. **187**, 111 (1994).
[6] E. Mariotti, M. Meucci, P. Bicchi, C. Marinelli, and L. Moi, Opt. Commun. **134**, 121 (1997).
[7] M. Allegrini, P. Bicchi, L. Moi, and P. Savino, Opt. Commun. **32**, 396 (1980).
[8] E. Mariotti, J. H. Xu, M. Allegrini, G. Alzetta, S. Gozzini, and L. Moi, Phys. Rev. A **38**, 1327 (1988).
[9] A. N. Nesmeyanov, *Vapor Pressure of the Chemical Elements* (Elsevier, Amsterdam, 1963).
[10] R. J. Borg and G. J. Dienes, *An Introduction to Solid State Diffusion* (Academic, Cambridge, 1988).